

Frequency based mapping of the *STN* borders

Konrad A. Ciecierski¹, Zbigniew W. Ras^{2,1}, and Andrzej W. Przybyszewski³

¹ Warsaw Univ. of Technology, Institute of Comp. Science, 00-655 Warsaw, Poland

² Univ. of North Carolina, Dept. of Comp. Science, Charlotte, NC 28223, USA

³ UMass Medical School, Dept. of Neurology, Worcester, MA 01655, USA

K.Ciecierski@ii.pw.edu.pl, ras@uncc.edu,

Andrzej.Przybyszewski@umassmed.edu

Abstract. During deep brain stimulation (DBS) surgery for Parkinson disease, the target is the subthalamic nucleus (*STN*). *STN* is small, (9 x 7 x 4 mm) and typically localized by a series of parallel microelectrodes. As those electrodes are in steps advanced towards and through the *STN*, they record the neurobiological activity of the surrounding tissues. By careful inspection and analysis of such recordings one can obtain a range of depth at which given electrodes passed through the *STN*. Both human made inspection and computer based analysis are performed during surgery in the environment of the operation theatre. There are several methods for the *STN* detection, one of them – developed by the authors – is described in [8]. While the detection of the *STN* interior can be obtained with good certainty its borders can be slightly fuzzy and sometimes it is difficult to classify whether given depth should be regarded as belonging to the *STN* proper or lying outside of it. Mapping of the borders is important as the tip of the final permanent stimulating electrode is often placed near the ventral⁴ border of the *STN* [12]. In this paper we are showing that analysis focusing on narrow frequency bands can yield better discrimination of the *STN* borders and *STN* itself.

Keywords: *STN* border, DBS, Wavelet, DWT decomposition, Band filtering, Signal power

Introduction

The first line of treatment for Parkinson Disease (PD) is pharmacological one. Still, some patients do not tolerate the anti PD drugs very well, in some others with time the effectiveness of treatment lessens and the dosage has to be gradually increased. This might eventually lead to motor fluctuations between ON

⁴ bottom

and OFF states [4]. For some of those patients, the surgical treatment can be applied as an alternative to ineffective pharmacological one. This treatment is called the Deep Brain Stimulation. During the surgery, in specific part of the brain the permanent stimulating electrodes are placed [4]. The technical problem of this surgery is that the target within which the electrodes are to be placed – Subthalamic Nucleus (*STN*) – is small and difficult to precisely locate using conventional medical imaging techniques i.e. CT⁵ and MRI⁶.

In the literature and in medical practice there are several approaches to localization of the *STN*. Some of them are purely CT and MRI based while others rely for example on intrasurgical microrecording [11][10]. Microrecording localization is based on the fact that *STN* has a physiology that is distinct from this of adjacent brain territories [4][3].

In microelectrode based methods, during surgery several thin parallel electrodes are inserted into patient’s brain and in measured steps advanced towards and through the *STN*. The electrodes, as they advance through the brain, at each step perform typically a 10s long recording of the activity of the brain tissue surrounding their recording tips. *STN* is characterized by high neuronal activity [3] and due to pathological changes that occur in PD, the activity of the *STN* is even more increased [4]. By this, using carefully designed computer analysis one can discriminate between recordings that have been registered within the *STN* and outside of it. Mapping of the interior part of the *STN* is by this achieved with reliable and repeatable results. Of course there are border cases with recordings registered at the dorsal⁷ and ventral⁸ borders of the *STN*. Those borders may differ from patient to patient, sometimes they are clearly defined in the span of single millimeter while in other cases they might be fuzzed over few millimeters. One might now ask, why the precise localization of the borders is so important as long as one can safely map the interior of the *STN*.

Best results with least risk of complications are achieved when the tip lead of the stimulating electrode is located close to the ventral border of the *STN* [4]. In this way, contacts of the electrode that are above its tip are still within the *STN* and close to its ventral border.

1 Band power calculation

In previously published papers [5]–[9] we computed the signal’s power for two distinct frequency ranges, i.e. LFB for frequencies below 500 Hz and HFB for frequencies between 500 Hz and 3 KHz. Both attributes – even alone – provide reasonably good discrimination between *STN* and non *STN* recordings. As shown in Table 1, the ranges of Q1 – Q3 quartiles do not overlap for either of them.

⁵ Computer Tomography

⁶ Magnetic Resonance Imaging

⁷ top

⁸ bottom

Table 1. Electrode rank example

Attribute	Class	Q1	Q2	Q3
LFB	$\neg STN$	0.833	1.034	1.392
	STN	2.253	3.644	5.775
HFB	$\neg STN$	0.922	1.063	1.429
	STN	2.650	4.103	6.272

Still, for the 25% of the STN recordings their LFB and HFB are lower than respectively provided Q1 values. Those cases are in some cases related to patients with unusually quiet STN or simply are border cases recorded at the dorsal or ventral borders of the STN .

For any function that can be calculated for data recorded in course of a single electrode at consecutive depths, there is a need for normalization. This procedure is described in detail in [8]. Here we will only mention, that in this procedure, average from the first five depth is treated as a base value and values of that function taken from all depths for that electrode are divided by this base value.

An example of the normalized LFB (Low Frequency Background power [8][9]) value calculated for a PD patient with unusually quiet STN is presented on Fig. 1.

Only at two depths the value of the LFB attribute was above 3 and never on the whole track of the electrode it exceeded 4. This electrode was also the best one as other two electrodes provided even worse STN localization.

The classifier pinpointed the depths -1000 μm and 0 μm as belonging to the STN . Due to the sheer drop of the LFB at +1000 μm it was assumed that at depth 0 μm is the ventral border of the STN . Problematic however was the localization of the dorsal STN border. Does it start at -1000 μm or maybe earlier at -3000 μm . During test stimulations performed in the course of the surgery the STN extent has been mapped to be between -2000 μm and 0 μm .

This means that depth at -2000 μm has not been correctly mapped as STN and this contributed to the lowering of the sensitivity of the classification.

2 Narrow band power calculation

Power calculated summarily for range below 500 Hz (LFB) was clearly not sufficient to fully identify the extent of the STN in the case described above.

What would be the result if one were to cut the power spectrum in much narrower bands.

To obtain power calculation for narrow frequency bands, the recorded signals were DWT fully transformed i.e. both in low and high frequencies [1][2]. Recorded signals are sampled with 24 KHz and have 10 s lengths. For DWT applicability the signals were zero padded to closest length being the power of 2 i.e. 262144 samples. DWT was then performed up to level where single set of coefficients

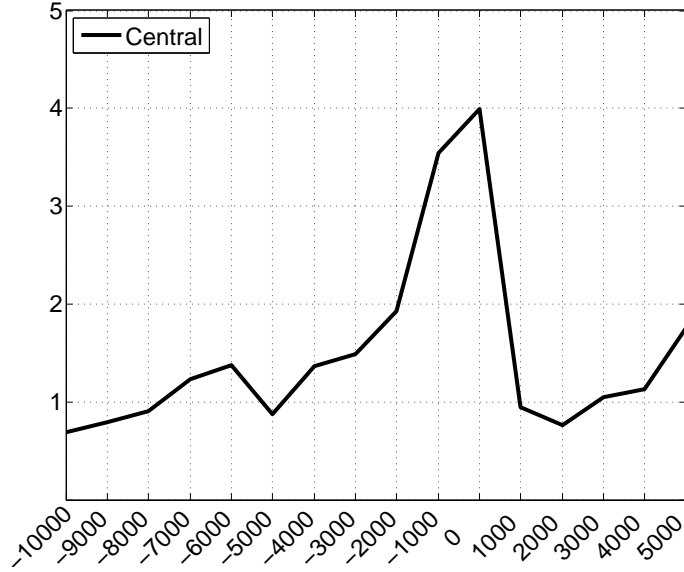


Fig. 1. Low value of LFB obtained from quiet *STN*

had 64 elements and represented frequency span of about 3 Hz. In this way the frequency range was evenly split into \mathcal{F}_{DIV} set of 4096 consecutive intervals .

For given frequency range g its coverage $\mathcal{F}_{COV}(g)$ is defined as

$$\mathcal{F}_{COV}(g) = \{f : f \in \mathcal{F}_{DIV} \wedge \frac{\overline{f \cap g}}{\overline{f}} \geq \frac{1}{2}\}$$

If for given depth d and $f \in \mathcal{F}_{DIV}$, computed set of DWT coefficients is denoted as $DWT_c(d, f)$ then power calculated for given frequency range g is

$$PWR(d, g) = \sum_{f \in \mathcal{F}_{COV}(g)} \sum_{x \in DWT_c(d, f)} x^2$$

When one is now to regard the signal's power in various frequency bands some clear differences might be noticed. In selected frequency bands different parts of the *STN* are clearly more active then in others. Normalized powers for the same electrode are shown on Fig. 2 as in Fig. 1 but in two selected frequency bands.

Unfortunately this finding cannot be generalized. In some patients given frequency range is characteristic for a given part of *STN* while in others this range is completely different – to the point that they do not even overlap. There is a saying that there are not two identical cases of Parkinson Disease, just the same there are no two identical brains and subthalamic nucleuses. Even left and right *STN* in the same patient present different frequency characteristics. Power percentiles calculated from 4138 *STN* recordings registered during 173 surgeries

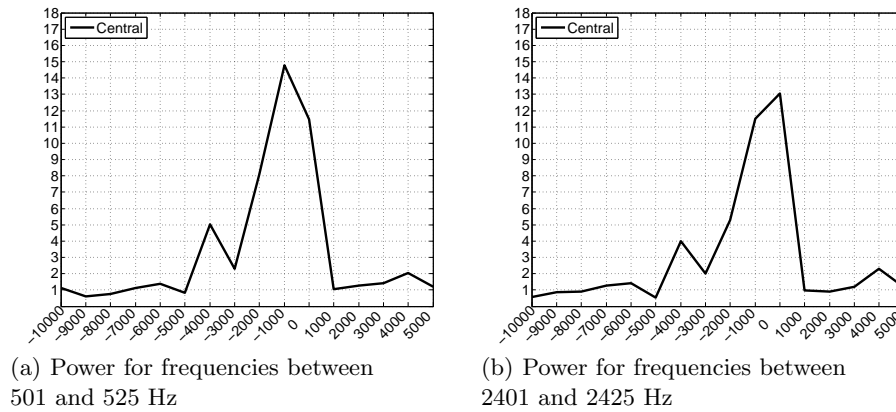


Fig. 2. Power for frequency bands

are shown on Fig. 3 below. Calculations were made for consecutive, 25 Hz wide frequency ranges below 3 KHz.

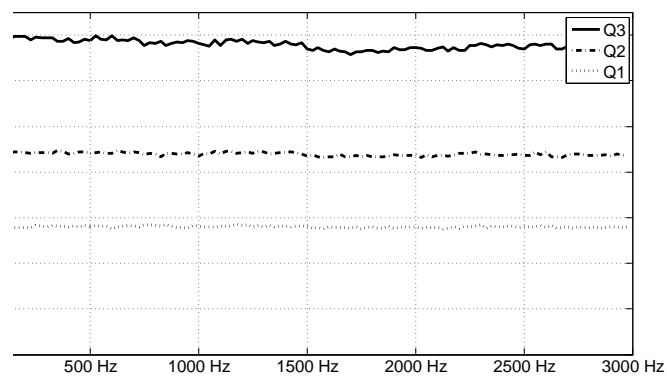
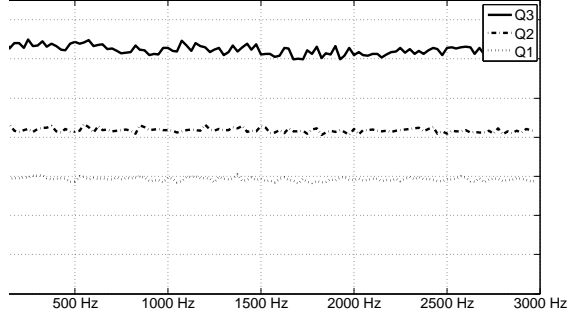


Fig. 3. Power quartile distribution over frequencies for STN recordings

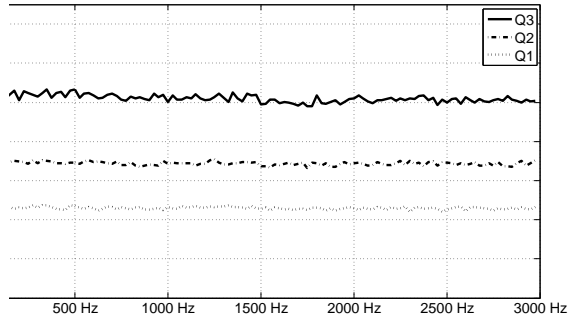
It is immediately evident that no frequency is patients-wide characteristic for the *STN*.

Some general anatomically based frequency findings can still however be found. When above distribution is calculated not for all STN recordings but separately for those from dorsal and ventral borders of the STN differences are clearly present as shown on Fig. 4(a) and 4(b).

While power is still almost evenly distributed among frequencies, the dorsal parts of the STN gave recordings yielding greater power than ventral ones.



(a) Power quartile distribution over frequencies for dorsal STN recordings



(b) Power quartile distribution over frequencies for ventral STN recordings

Fig. 4. Power quartile distribution for recordings from parts of the STN

3 Narrow band power based discriminating attribute

From the previous section it is evident that various parts of the STN display different frequency characteristics and that those characteristics are highly individual and cannot be easily generalized. As all recordings were made with high impedance electrodes, using low impedance electrodes one may find frequencies that do carry significantly more power in certain STN areas [12].

In any given patient for any part of the STN we can however find a frequency range at which its normalized power is minimized or maximized. Thus for any given depth we can compute minimal and maximal normalized narrow band power.

$$PWR_{MIN}(d) = \min_{f \in \mathcal{F}_{DIV}} PWR(d, f)$$

$$PWR_{MAX}(d) = \max_{f \in \mathcal{F}_{DIV}} PWR(d, f)$$

Such attributes maximize and minimize the power calculated for given depth regardless at which frequency brain tissue located there is most and least active. This should help discriminate the border cases and help in more finetuned STN border mapping.

For electrode pass shown on Fig. 2 the PWR_{MAX} is shown on Fig. 5. This time value of PWR_{MAX} beside obvious increase at $-1000 \mu m$ and $0 \mu m$ is also more elevated at depth $-2000 \mu m$. That is depth which was classified by the neurosurgeon as belonging to the STN and misclassified by the algorithm given in [8][9].

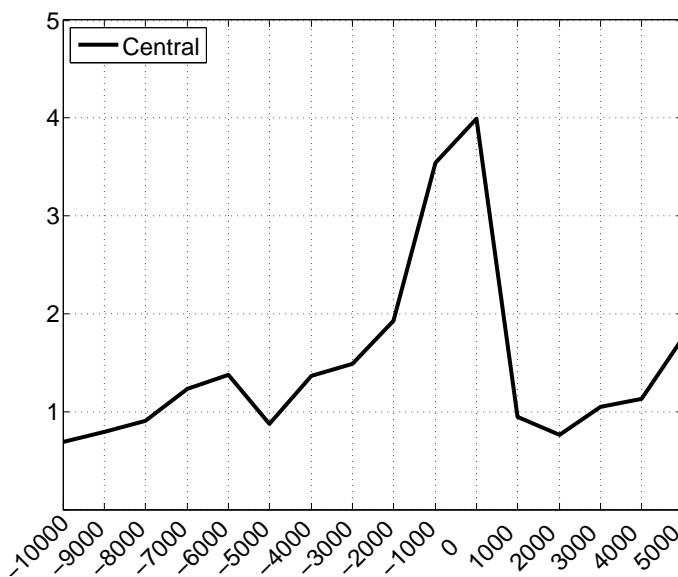


Fig. 5. PWR_{MAX} obtained from quiet STN

4 Evaluation

For evaluation purposes a test set of 14422 recordings was used. Those recordings were registered during 135 neurosurgeries. The attributes used in set were based both on spike occurrence and background neural activity. They are described in detail in [8][9].

The 10-fold cross validation results obtained with Random Forest classifier are shown in Table 2

$$sensitivity = \frac{3061}{3061+189} \approx 0.942 \quad specificity = \frac{11054}{11054+118} \approx 0.989$$

Table 2. Cross validation results

		Human classification		Total
		<i>STN</i>	<i>MISS</i>	
Classifier	<i>STN</i>	3061	118	3179
	<i>MISS</i>	189	11054	11243
Total		3250	11172	14422

When existing attributes were extended by the PWR_{MIN} and PWR_{MAX} attributes the results are similar regarding specificity but clearly better in sensitivity. That means that in this configuration classifier has recognized properly more of the *STN* recordings. Count of false negatives dropped from 189 to 160.

Table 3. Cross validation results

		Human classification		Total
		<i>STN</i>	<i>MISS</i>	
Classifier	<i>STN</i>	3090	133	3223
	<i>MISS</i>	160	11039	11199
Total		3250	11172	14422

$$sensitivity = \frac{3090}{3090+160} \approx 0.951 \quad specificity = \frac{11039}{11039+133} \approx 0.988$$

Many of those corrected false negatives represented recordings from unusually quiet *STNs* or described earlier cases of dorsal or ventral *STN* borders. Among them is also – described in Section 1 – corrected misdetection of the *STN* at $-2000 \mu m$.

When existing background based attributes [8] were replaced by the set of attributes representing normalized power calculated for \mathcal{F}_{DIV} frequency intervals, the results became slightly worse.

Table 4. Cross validation results

		Human classification		Total
		<i>STN</i>	<i>MISS</i>	
Classifier	<i>STN</i>	2968	152	3120
	<i>MISS</i>	282	11020	11302
Total		3250	11172	14422

$$sensitivity = \frac{2968}{2968+282} \approx 0.913 \quad specificity = \frac{11020}{11020+152} \approx 0.986$$

Both the false positive and false negative counts have increased. Clearly unsegregated power values calculated for \mathcal{F}_{DIV} cannot provide as good discrimination as normalized power calculated for two specific wide frequency ranges i.e. below 500 Hz and between 500 Hz and 3 KHz.

Finally, if one were to build classifier solely on those \mathcal{F}_{DIV} based attributes the results are much worse.

Table 5. Cross validation results

		Human classification		Total
		<i>STN</i>	<i>MISS</i>	
Classifier	<i>STN</i>	2382	452	2834
	<i>MISS</i>	868	10720	11588
Total		3250	11172	14422

$$sensitivity = \frac{2382}{2382+868} \approx 0.733 \quad specificity = \frac{10720}{10720+452} \approx 0.960$$

The sensitivity has dropped from 0.989 to 0.733 while the specificity has increased from 0.942 to 0.960. The dramatic decrease of sensitivity proves that while \mathcal{F}_{DIV} based aggregative attributes do improve classification, they themselves alone in their plain form are insufficient for good classification.

5 Summary

Methods described in [8][9] provide good basis for discrimination between STN and non STN recordings. The quality of the classification has been repeatedly confirmed during many neurosurgeries performed at Institute of Psychiatry and Neurology in Warsaw.

In some cases the classifier still fails to correctly identify a recording registered within the STN. This, in most cases comes from one of the two possible causes:

- Patient has STN with unusually low activity
- Wrongly classified location lies on border between STN and another adjacent brain area

While STN may be misdetected due to either one of the above causes or both of them, one might still often find its increased activity at certain frequency ranges. Problem lies in natural individuality of brain functioning as well as in individuality of Parkinson Disease related pathological disturbances in its physiology [3].

Using high impedance recording microelectrodes no narrow frequency band could have been found such that its elevated power would be STN characteristic

for majority of the patients. Increase of signal's power quartiles within STN is evident for all frequency sub bands below 3 KHz.

Still, while it is hard to say which frequency range at which part of the STN should yield increased power, one might hypothesize that at least for some of those frequency bands the power indeed would be increased. That hypothesis led to construction of the PWR_{MIN} and PWR_{MAX} attributes that reflect lowest and highest band based power obtained from given recording.

During classification tests, use of those two additional attributes improved the sensitivity which has increased from 0.942 to 0.951 While the increase by ≈ 0.01 might seem to be small, it is nonetheless important as it improves classification of the most difficult cases.

References

1. A.Jensen, A Ia Cour-Harbo. Ripples in Mathematics, Springer-Verlag, 2001
2. S.W. Smith. Digital Signal Processing, Elsevier, 2003
3. J. Nolte. The Human Brain, An Introduction to Its Functional Anatomy, 2009
4. Z. Israel, K. J. Burchiel. Microelectrode Recording in Movement Disorder Surgery, Thieme Medical Publishers, 2004
5. K. Ciecierski, Z. W. Raś, A. W. Przybyszewski, Foundations of recommender system for STN localization during DBS surgery in Parkinson's patients, Foundations of Intelligent Systems, ISMIS 2012 Symposium, LNAI, Vol. 7661, Springer, 2012, 234–243
6. K. Ciecierski, Z. W. Raś, A. W. Przybyszewski, Discrimination of the micro electrode recordings for STN localization during DBS surgery in Parkinson's patients, Flexible Query Answering Systems, FQAS 2013 Symposium, LNAI, Vol. 8132, Springer, 2013, 328–339
7. K. Ciecierski, Z. W. Raś, A. W. Przybyszewski, Foundations of automatic system for intrasurgical localization of subthalamic nucleus in Parkinson patients, Web Intelligence and Agent Systems, 2014/1, IOS Press, 2014, 63–82
8. K. Ciecierski, Decision Support System for surgical treatment of Parkinsons disease, PhD thesis, Warsaw University of technology Press, 2013
9. K. Ciecierski, T. Mandat, R. Rola, Z. W. Raś, A. W. Przybyszewski Computer aided subthalamic nucleus (STN) localization during deep brain stimulation (DBS) surgery in Parkinson's patients, Annales Academiae Medicae Silesiensis, 2014, 68, 5: 275-283
10. T. Mandat, T. Tykocki, H. Koziara et. al. Subthalamic deep brain stimulation for the treatment of Parkinson disease, Neurologia i neurochirurgia polska 45.1 (2011): 32-36
11. P. Novak, A. W. Przybyszewski, A. Barborica, P. Ravin, L. Margolin, J. G. Pilitis Localization of the subthalamic nucleus in Parkinson disease using multiunit activity, Journal of the neurological sciences 310.1 (2011): 44-49.
12. A. Zaidel, A. Spivak, L. Shpigelman, H. Bergman, and Z. Israel Delimiting subterritories of the human subthalamic nucleus by means of microelectrode recordings and a Hidden Markov Model, Movement disorders 24, no. 12 (2009): 1785-1793.